Heart Rate Turbulence Analysis Based on Photoplethysmography

Eduardo Gil*, Pablo Laguna, *Senior Member, IEEE*, Juan Pablo Martínez, Óscar Barquero-Pérez,
Arcadi García-Alberola, and Leif Sörnmo, *Senior Member, IEEE*

Abstract—The goal of this paper is to determine whether the photoplethysmography (PPG) can replace the ECG-based detection of heart rate turbulence. Using the PPG, classification of ventricular premature beats (VPBs) is accomplished with a linear classifier. The two conventional parameters turbulence onset and slope are studied together with a recently introduced parameter characterizing turbulence shape. Performance is studied on a dataset with 4131 VPBs, recorded from a total of 27 patients in different clinical contexts (hemodialysis treatment, intensive care monitoring, and electrophysiological study). The sensitivity/specificity of VPB classification was found to be 90.5/99.9%, with an accuracy of 99.3%, suggesting that classification of VPBs can be reliable made from the PPG. The main difference between the two types of turbulence analysis stems from the fact that the pulse transit time varies largely immediately after the VPB. Out of the 22 patients which had a sufficient number of VPBs, the outcome of the ECG- and PPG-based analysis was identical in 21. It is concluded that the PPG may serve as a surrogate technique for the ECG in turbulence analysis.

Index Terms—Heart rate turbulence (HRT), hemodialysis, photoplethysmography (PPG), pulse rate turbulence (PRT), pulse transit time (PTT), ventricular premature beat (VPB).

*E. Gil is with the Communications Technology Group (GTC), Aragón Institute of Engineering Research (I3A), Universidad de Zaragoza, 50004 Zaragoza, Spain, and also with the Centro de Investigación Biomédica en Red en Bioingeniería, Biomateriales y Nanomedicina (CIBER-BBN), 50018 Zaragoza, Spain (e-mail: edugilh@unizar.es).

P. Laguna and J. P. Martínez are with the Communications Technology Group (GTC), Aragón Institute of Engineering Research (I3A), Universidad de Zaragoza, 50004 Zaragoza, Spain, and also with the Centro de Investigación Biomédica en Red en Bioingeniería, Biomateriales y Nanomedicina (CIBER-BBN), 50018 Zaragoza, Spain (e-mail: laguna@unizar.es; jpmart@unizar.es).

Ó. Barquero-Pérez is with the Department of Signal Theory and Communications, Rey Juan Carlos University, 28943 Madrid, Spain (e-mail: oscar.barquero@urjc.es).

A. García-Alberola is with the Arrhythmia Unit, Hospital Universitario Virgen de la Arrixaca de Murcia, 30008 Murcia, Spain (e-mail: arcadi@secardiologia.es).

L. Sörnmo is with the Department of Electrical and Information Technology and Center of Integrative Electrocardiology, Lund University, 22100 Lund, Sweden (e-mail: leif.sornmo@eit.lth.se).

Color versions of one or more of the figures in this paper are available online at http://ieeexplore.ieee.org.

Digital Object Identifier 10.1109/TBME.2013.2270083

I. INTRODUCTION

HEART rate turbulence (HRT) refers to a short-term fluctuation in the heart rate, triggered by a ventricular premature beat (VPB) [1], [2]. Such turbulence is considered to be a blood pressure regulating mechanism which, in normal subjects, compensates for the VPB-induced drop in the blood pressure by an initial, accelerated sinus rate. The heart rate then decelerates, causing an overshoot in its response, and returns to the baseline; the blood pressure returns to its preextrasystolic level. In normal subjects, the presence of HRT can be detected and characterized once ensemble averaging of several VPB-aligned RR interval series has first been performed to provide a more stable estimate than does the series of a single VPB. Blunted or missing HRT reflects autonomic dysfunction and is associated with various conditions. In particular, HRT has been established as a powerful risk predictor of mortality and sudden cardiac death following acute myocardial infarction [1], [3], [4], but HRT has also been found useful to study in many other clinical applications, for example, in patients with congestive heart failure and diabetes mellitus [5].

The frequent occurrence of VPBs in dialysis patients renders it possible to compute parameters which characterize HRT [6]. Since autonomic neuropathy is known to be associated with a marked fall in the blood pressure during hemodialysis, HRT may convey clinical information in those patients [7]. To date, one study has addressed the issue whether higher propensity to intradialytic hypotension is reflected by HRT [8]. The results showed that the acceleration in heart rate that follows a VPB is significantly lower in patients prone to intradialytic hypotension than in resistant patients. Using ambulatory ECG recordings, Celik *et al*. [9] studied changes in the conventional HRT parameters before and after hemodialysis treatment, but not during treatment. The parameters were found to be significantly blunted in all patients, although they were not affected by hemodialysis treatment.

From a clinical viewpoint, ECG monitoring is not commonly performed during hemodialysis because of the inconvenience to wear the ECG electrodes [10]. Considering that pulse oximetry, thanks to its ease of use, was recently employed for online monitoring during hemodialysis [11], [12], it is of considerable interest to study whether the photoplethysmography (PPG) can serve as a surrogate technique for the ECG when characterizing HRT. PPG-based analysis is, however, challenged by a signal which is quite vulnerable to motion artifacts. For example, artifacts caused by arm movements may compromise the analysis accuracy when the PPG sensor is attached to the nonfistula arm during hemodialysis [10], [13]. Several methods have been

developed for artifact detection [14]–[16], and some also for the reduction of noise and artifacts [17].

The goal of this paper is to investigate whether the PPG can serve as a surrogate technique for the ECG in HRT analysis. To test this hypothesis, both numerical and categorical studies have been performed, using HRT derived from the ECG as the reference in all cases. Since the analysis should be fully automated, it is necessary to first develop a PPG-based method for VPB classification; the few efforts described in the literature on PPG-based analysis of VPBs have been performed manually [18].

This paper is organized as follows. Section II describes the annotated databases used for performance evaluation. Section III presents the approach taken to PPG-based VPB detection and classification, and describes the related analysis of HRT, which in the following is referred to as pulse rate turbulence (PRT). Performance is evaluated in Section IV by comparing the results from PPG- and ECG-based analysis. Special attention is paid to the influence of pulse transit time (PTT) on different turbulence parameters.

II. DATA

The data used for performance evaluation were selected from patients in three clinical contexts, namely, hemodialysis treatment, intensive care monitoring, and electrophysiological (EP) investigation. The ECG served as "gold standard" for evaluating VPB classification performance and PRT characterization.

A. Hemodialysis Database

Eleven patients with end-stage renal disease, classified as hypotension prone by a nephrologist, participated in the study. The patients underwent regular hemodialysis treatment thrice a week at Rigshospitalet, Copenhagen. Data were acquired continuously during treatment, which lasted from 3 to 5 h. The dialysis machines Gambro AK 200 or AK 200 Systems (Gambro Lundia AB, Sweden) were used for treatment. The dialyzer filters were selected according to each patient's individual requirements; for further details, see [12]. The three ECG leads V_1, V_5, and II were acquired using the Biopac ECG100C amplifier, sampled at a rate of 1000 Hz with the Biopac MP150 data acquisition system (BIOPAC Systems Inc., Goleta, CA, USA). The PPG signal was acquired with a pulse oximeter (LifeSense R, Medair AB, Sweden), also sampled at a rate of 1000 Hz with the Biopac MP150. This database was used for developing and evaluating the VPB classifier, see Section III-B.

B. MIMIC Database

The multiparameter intelligent monitoring in intensive care (MIMIC) database was acquired from a large number of patients in intensive care units of Beth Israel Deaconess Medical Center, Boston, MA, USA, and includes signals as well as data from the patients' medical records [19]. The database contains a wide range of clinical classes, including hemodynamically unstable patients. The ECG and PPG signals were originally sampled at rates of 500 and 125 Hz, respectively, but digitally interpolated

TABLE I
NUMBER OF VPBs FOR EACH PATIENT

Hemodialysis		MIMIC		EP study	
Patient	#VPBs	Patient	#VPBs	Patient	#VPBs
H1	39	M1	429	A1	28
H2	24	M2	484	A2	29
H3	31	M3	629	A3	39
H4	349	M4	562	A4	9
H5	3	M5	359	A5	27
H6	9	M6	396	A6	13
H7	319			A7	20
H8	14			A8	36
H9	28			A9	27
H10	147			A10	31
H11	50				

to a sampling rate of 1000 Hz in order to match the time resolution of the other two databases as well as to comply with the recommendations in [20].

C. EP Database

VPBs were induced in ten patients, with structurally normal hearts, during EP investigation at the Hospital Universitario Virgen de la Arrixaca, Murcia, Spain. The acquisition protocol was approved by the local ethics committee. The EP database was especially acquired for this paper to ensure that patients with pronounced HRT were also included, since the two aforementioned databases include patients with varying degrees of impaired autonomic function.

Sequences of VPBs were delivered under controlled conditions, and induced in sinus rhythm by cyclic pacing from the right ventricular apex after every 21 spontaneous beats. The 12-lead ECG was recorded with the LabSystem Pro EP System (Bard Inc., Murray Hill, NJ, USA), and the PPG was recorded with the Masimo Radical-7 pulse oximeter. Both types of signals were acquired at a sampling rate of 2000 Hz and decimated to 1000 Hz.

D. VPB Annotation and HRT Criteria Using the ECG

The annotation of VPBs was based on information derived from the ECG. Following wavelet-based QRS detection [21], VPBs were determined from information on rhythm and beat morphology [22]. VPBs were excluded from further analysis when either excessive noise was present in the ECG or PPG signals (visually identified) or when other VPBs occurred within the 5 previous or 20 subsequent beats.

Table I presents the number of VPBs for each patient of the three databases which were subjected to analysis. At least 20 VPBs were required for turbulence analysis, resulting in a total of 22 patients.

III. METHODS

A. PPG Pulse Types

Different pulse patterns can be discerned in the PPG signal when a VPB occurs [18]. Depending on the degree of blood pumping efficiency, the VPB may, or may not, be accompanied with a pulse. The following four pulse types are defined, of which the last three are VPB-related (see Fig. 1):
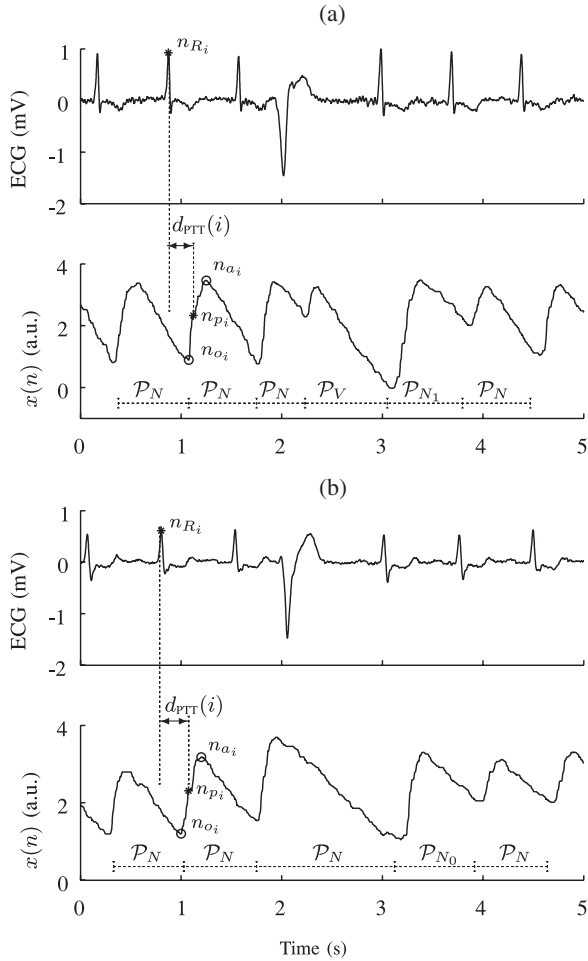
Fig. 1. Example of a VPB (a) with and (b) without an accompanying pulse in the PPG signal associated with the VPB. Note that $\mathcal{P}_V$ pulse does not exist in (b). Significant points are indicated that define the parameters for classification.

1) normal pulse associated with a normal beat ($\mathcal{P}_N$);
2) pulse associated with a VPB ($\mathcal{P}_V$);
3) normal pulse occurring immediately after a VPB which does not cause a pulse ($\mathcal{P}_{N_0}$);
4) normal pulse occurring immediately after a VPB which causes a pulse ($\mathcal{P}_{N_1}$). Note that $\mathcal{P}_{N_1}$ always follows a pulse of type $\mathcal{P}_V$.

The "binary" classification problem was also studied in which the three VPB-related pulse types, i.e., $\mathcal{P}_V$, $\mathcal{P}_{N_0}$, and $\mathcal{P}_{N_1}$ were merged into one type, denoted $\mathcal{P}_{VN}$.

The pulse type $\mathcal{P}_V$ was manually annotated in the hemodialysis database and used as a training set; a total of 201 pulses were annotated. Normal pulses surrounding a VPB—three preceding and ten following—were also annotated, resulting in 812 $\mathcal{P}_{N_0}$, 201 $\mathcal{P}_{N_1}$, and 13169 $\mathcal{P}_N$. Note that the numbers of $\mathcal{P}_V$ and $\mathcal{P}_{N_1}$ are always identical, and that the number of $\mathcal{P}_N$ is given by $(3 + 10) \cdot (812 \mathcal{P}_{N_0} + 201 \mathcal{P}_{N_1}) = 13169$.

B. PPG-Based Classification of VPBs

Noise in the PPG signal is reduced by a finite impulse response low-pass filter with cutoff frequency at 35 Hz; the filtered

PPG signal is denoted $x(n)$. The onset n_{o_i} and apex location n_{a_i} of the ith pulse are determined once the zero-crossing of the derivative of $x(n)$ is located.

Three simple pulse parameters are studied which characterize upslope/downslope pulse amplitude

$$a_+(i) = x(n_{a_i}) - x(n_{o_i}) \tag{1}$$

$$a_-(i) = x(n_{a_i}) - x(n_{o_{i+1}}) \tag{2}$$

and the apex-to-apex interval

$$d_{aa}(i) = n_{a_i} - n_{a_{i-1}}. \tag{3}$$

This interval definition is well suited for all pulse types, including intervals with mixed pulse types. A more precise pulse-to-pulse interval definition is introduced in the next section where the analysis is confined to normal pulses.

The feature set used for classification of the ith pulse also includes the parameters of the previous pulse in order to account for the close relationship between $\mathcal{P}_V$ and $\mathcal{P}_{N_1}$. Thus, the investigated feature set is defined by

$$\{a_+(i), a_-(i), d_{aa}(i), a_+(i-1), a_-(i-1), d_{aa}(i-1)\}. \tag{4}$$

Prior to classification, all features are normalized with their respective mean values computed from the five preceding normal pulses. Linear discriminant analysis is employed for VPB classification, where the discriminant function is evaluated for each pulse type. The ith pulse is assigned to that pulse type $\mathcal{P}_N$, $\mathcal{P}_V$, $\mathcal{P}_{N_0}$, and $\mathcal{P}_{N_1}$, which produces the largest value [23].

The wrapper-based forward approach was used for feature selection in which each step of the procedure adds that feature which improves performance accuracy the most. Cross validation was then used for performance evaluation. A confusion matrix was determined for each subject by comparing the classifier outcome with the annotation of all pulses of the training set, except for those of the current subject. Finally, the classifier confusion matrix was computed by accumulating the confusion matrices of all subjects. The different pulse types were balanced in the training process so that the same weight could be assigned to all types, regardless of their prior probability.

C. Pulse Rate Turbulence

The PRT analysis requires that a fiducial point of the pulse is defined so that the interval series can be aligned to the fiducial point of other VPBs, and then subjected to ensemble averaging (similar to HRT analysis). Although the pulse onset n_{o_i} or the apex location n_{a_i} may both serve as fiducial point, the time for half the pulse amplitude defined by

$$n_{p_i} = \arg \min_{n \in [n_{o_i}, n_{a_i}]} \left(x(n) - \frac{x(n_{o_i}) + x(n_{a_i})}{2} \right) \tag{5}$$

is employed due to a smaller localization error than for n_{a_i} [24]. The pulse-to-pulse interval series, denoted $d_{pp}(i)$, that follows the VPB is, therefore, determined from the intervals defined by n_{p_i} (see Fig. 1).

In this paper, turbulence is characterized not only by turbulence onset (TO) and turbulence slope (TS) but also by the novel shape parameter T_Σ [25]. The latter parameter is based on

the extended integral pulse frequency modulation model, and uses second-order statistics for characterizing the signal subspace, defined by the three most significant functions of the Karhunen–Loève (KL) transform. The KL basis applied here was previously determined from a population of 90 patients with ischemic cardiomyopathy and mild-to-moderate congestive heart failure [25]. Thus, the KL basis is not matched to the databases of this paper.

D. Pulse Transit Time

The PTT is computed for the purpose of better understanding differences between the heart rate and pulse rate [26]. The PTT is defined as the time that elapses between the R wave peak, occurring at n_{R_i}, and the fiducial point of the related PPG pulse, occurring at n_{p_i}, i.e.,

$$d_{\mathrm{PTT}}(i) = n_{p_i} - n_{\mathrm{R}_i} \qquad (6)$$

(see Fig. 1). With the definition of the pulse-to-pulse interval as

$$d_{pp}(i) = n_{p_i} - n_{p_{i-1}} \qquad (7)$$

it is easily shown that pulse-to-pulse intervals and RR intervals are related through

$$d_{pp}(i) = d_{RR}(i) + \Delta d_{\mathrm{PTT}}(i) \qquad (8)$$

where $\Delta d_{\mathrm{PTT}}(i) = d_{\mathrm{PTT}}(i) - d_{\mathrm{PTT}}(i-1)$.

E. Performance Evaluation

The nonparametric Mann–Whitney U-test was applied to the $d_{pp}(i)$-based parameters TO, TS, and T_Σ for the purpose of evaluating their power to detect turbulence with the ECG-derived cutoff values. For TO and TS, turbulence was judged to be present when the conventional cutoff values were applied, i.e., 0% and 2.5 ms/beat, respectively [1]. For the shape parameter T_Σ, the cutoff value defined by the lower tertile of the population studied in [25] was applied, i.e., -0.75 arbitrary units. Note that these cutoff values must be adapted for each population in clinical applications.

Pearson's correlation coefficient ρ was determined for TO, TS, and T_Σ for quantifying the agreement between HRT and PRT analysis based on $d_{RR}(i)$ and $d_{pp}(i)$, respectively. Bland–Altman plots were also produced for characterizing the agreement. The performance of the PRT analysis was evaluated in terms of sensitivity (Se), specificity (Sp), and accuracy (Acc), using the HRT analysis as gold standard.

IV. RESULTS

A. PPG-Based Classification of VPBs

A classification accuracy of $Acc = 96.8\%$ was achieved for the four-class problem using the two temporal features $d_{aa}(i)$ and $d_{aa}(i-1)$ (see Table II). Classification based on all six features, i.e., including also $a_+(i), a_-(i), a_+(i-1), a_-(i-1)$, did not further improve accuracy since $Acc = 96.9\%$. Hence, VPB classification based on $d_{aa}(i)$ and $d_{aa}(i-1)$ was only considered.

TABLE II
(a) PERFORMANCE FIGURES AND (b) CONFUSION MATRIX
WHEN CLASSIFYING INTO FOUR DIFFERENT PULSE TYPES

(a)

	$\mathcal{P}_N$	$\mathcal{P}_V$	$\mathcal{P}_{N_1}$	$\mathcal{P}_{N_0}$
Se	97.1%	88.1%	87.1%	96.8%
Sp	96.0%	98.2%	99.0%	99.9%
Acc	97.0%	98.0%	98.8%	99.7%
Total Acc	96.8%			

(b)

Classifier output	Pulse types			
	$\mathcal{P}_N$	$\mathcal{P}_V$	$\mathcal{P}_{N_1}$	$\mathcal{P}_{N_0}$
$\mathcal{P}_N$	12781	24	22	2
$\mathcal{P}_V$	260	177	1	0
$\mathcal{P}_{N_1}$	118	0	175	24
$\mathcal{P}_{N_0}$	10	0	3	786

TABLE III
(a) PERFORMANCE FIGURES AND (b) CONFUSION MATRIX
WHEN CLASSIFYING INTO TWO DIFFERENT PULSE TYPES

(a)

	$\mathcal{P}_N$	$\mathcal{P}_{VN}$
Se	99.9%	90.5%
Sp	90.5%	99.9%
Acc	99.3%	99.3%
Total Acc	99.3%	

(b)

Classifier output	Pulse types	
	$\mathcal{P}_N$	$\mathcal{P}_{VN}$
$\mathcal{P}_N$	13159	96
$\mathcal{P}_{VN}$	10	917

Sensitivity, specificity, and accuracy when classifying either four or two pulse types are presented in Tables II and III, respectively, together with related confusion matrices. The aforementioned classification accuracy of $Acc = 96.8\%$ for four pulse types was found to increase to $Acc = 99.3\%$ when only two pulse types were considered. Note that the latter result on accuracy is the one that applies to PRT analysis.

B. Pulse Rate Turbulence

The two interval series $d_{RR}(i)$ and $d_{pp}(i)$ are displayed in Fig. 2 for a number of patients: two patients exhibiting pronounced turbulence and two patients completely lacking turbulence. It is obvious from these four cases that the agreement between $d_{RR}(i)$ and $d_{pp}(i)$ is good, except for the interval immediately after the VPB where the two series differ quite considerably. This difference may be explained by the term $\Delta d_{\mathrm{PTT}}(i)$ in (8) as a cause to the increase in $d_{pp}(i)$.

Fig. 3 presents boxplots of TO, TS, and T_Σ for turbulence (T) and nonturbulence (N) patients, computed from both $d_{RR}(i)$ and $d_{pp}(i)$. For $d_{RR}(i)$-based analysis, the T and N boxes are, by definition, separated by the parameter-specific cutoff values, so T and N groups are not necessarily the same for each parameter. The cutoff values were also applied to $d_{pp}(i)$-based analysis.

Statistical analysis of the $d_{pp}(i)$-based results showed that TO, TS, and T_Σ were all significantly different ($p < 0.001$) between T and N patients (see Fig. 3). When instead comparing the results of $d_{pp}(i)$-based analysis with the results of $d_{RR}(i)$-based analysis, no significant differences were found, neither
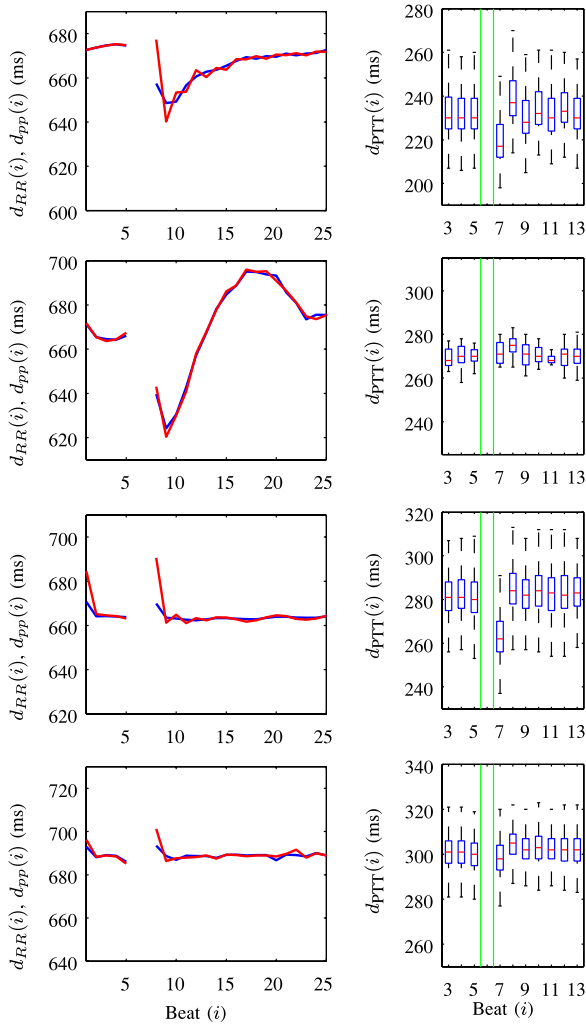
Fig. 2. RR intervals $d_{RR}(i)$ (blue line) and pulse-to-pulse intervals $d_{pp}(i)$ (red line) are displayed in the left column. Boxplots of the PTT $d_{\text{PTT}}(i)$ surrounding the VPBs are displayed in the right column. The results are displayed for patients M1, A7, M2, and M5 (top to bottom). The interval series have been subjected to VPB-aligned ensemble averaging.
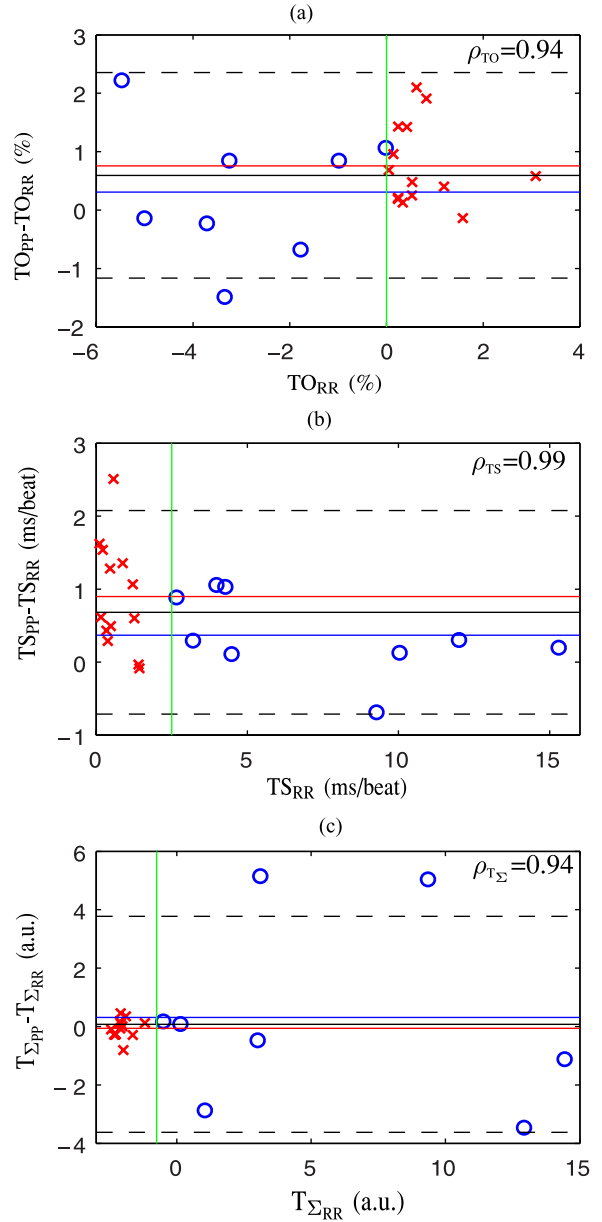

Fig. 3. Boxplots of TO, TS, and T_Σ for turbulence (T) and nonturbulence (N) patients, from analysis based on either $d_{RR}(i)$ or $d_{pp}(i)$. The cutoff value for each parameter is indicated with a horizontal dashed line. The character "§" indicates that the parameter is significantly different ($p < 0.001$) between turbulence (T) and nonturbulence (N) patients, and "$*$" indicates ($p < 0.05$) between $d_{RR}(i)$ and $d_{pp}(i)$.

Fig. 4. Bland–Altman plots (mean ± 1.96 std black solid and dashed lines) and correlation coefficients for the parameters (a) TO, (b) TS, and (c) T_Σ. The attached parameter index indicates whether $d_{RR}(i)$ or $d_{pp}(i)$ has been analyzed. The cutoff value (green line) distinguishes between T ("o") and N ("x") patients. The mean is indicated for T (blue line) and N patients (red line).
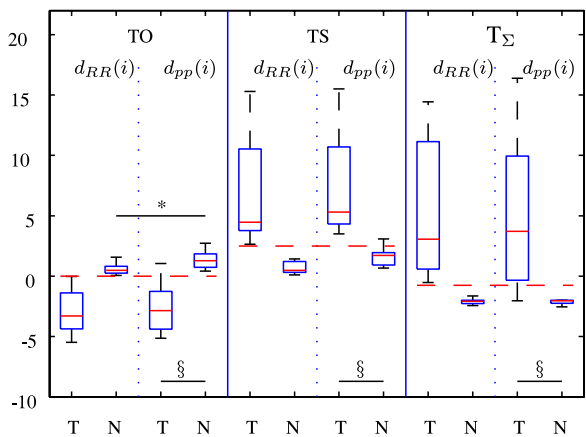
for T nor for N patients, except for TO which was significantly larger ($p < 0.05$) when computed from $d_{pp}(i)$ in N patients.

The Bland–Altman plots in Fig. 4, displaying the difference in results between $d_{pp}(i)$- and $d_{RR}(i)$-based analysis, indicate that bias is present in both TO and TS, but not in T_Σ. The main reason to the overestimation of TO and TS when analyzing $d_{pp}(i)$ is the influence of PTT—a finding which is discussed below. Correlation coefficients for each parameter are $\rho_{\text{TO}} = 0.94$, $\rho_{\text{TS}} = 0.99$, and $\rho_{T_\Sigma} = 0.94$. When analyzing only five VPBs in each recording rather than all VPBs, the correlation coefficients reduce to $\rho_{\text{TO}} = 0.89$, $\rho_{\text{TS}} = 0.92$, and $\rho_{T_\Sigma} = 0.77$.

TABLE IV
CLASSIFICATION RESULTS FOR THE PARAMETERS TO, TS, AND T$_\Sigma$

		TO$_{RR}$		Se	1
		N	T	Sp	0.88
TO$_{pp}$	N	14	1	Acc	0.95
	T	0	7		

		TS$_{RR}$		Se	0.92
		N	T	Sp	1
TS$_{pp}$	N	12	0	Acc	0.95
	T	1	9		

		T$_{\Sigma RR}$		Se	1
		N	T	Sp	0.88
T$_{\Sigma pp}$	N	14	1	Acc	0.95
	T	0	7		

The attached parameter index indicates whether $d_{RR}(i)$ or $d_{pp}(i)$ has been analyzed.

Classification performance and confusion matrices are presented in Table IV for $d_{pp}(i)$-based analysis with all VPBs. For the 22 patients, both types of analysis were found to produce the same results with respect to T/N outcome, except in one case. Patients with discrepant results were H1 for TO, M5 for TS, and M1 for T$_\Sigma$.

V. DISCUSSION

To the best of our knowledge, this is the first time VPB-induced perturbations in the cardiovascular system are studied in terms of information derived from the PPG signal. The characteristics of PRT, as well as of PTT in the presence of a VPB, were studied on three databases with widely different clinical origin.

A. VPB Classification

Although VPB classification is rendered difficult by the fact that a VPB may, or may not, be accompanied by a PPG pulse, an accuracy as high as $Acc = 96.8\%$ was achieved when classifying into four classes (see Table II), and $Acc = 99.3\%$ for two classes (see Table III). These results, achieved for two simple pulse features and a linear classifier, suggest that VPBs can be reliably detected from the PPG. For classification of pulse type, the apex-to-apex interval $d_{aa}(i)$ was employed since Acc was found to be 5% better with $d_{aa}(i)$ than with $d_{pp}(i)$ for four-class classification. The use of $d_{pp}(i)$ was, however, preferred over $d_{aa}(i)$ for the PRT analysis due to its more stable fiducial point definition [24]; in addition, a difference of only 0.1% in favor of $d_{aa}(i)$ was observed when classifying into two instead of four classes.

The inclusion of pulse amplitude features did not improve classification performance significantly. The main reason is that the amplitude features are correlated with the temporal features, which may be explained as follows. When $d_{pp}(i)$ increases, e.g., during a compensatory pause, the downslope amplitude $a_-(i)$ or the upslope amplitude $a_+(i+1)$ of the following pulse will also increase (cf., Fig. 1).

B. Turbulence Analysis

The turbulence patterns in $d_{RR}(i)$ and $d_{pp}(i)$ were almost identical in shape, as illustrated by Fig. 2. However, Fig. 2 also shows that PTT causes an increased variability in $d_{pp}(i)$ since the heart, after the compensatory pause, is filled with more blood than usual. This observation implies that the beat occurring immediately after a VPB is associated with a higher pressure which, in turn, causes the pulse wave to travel faster, as reflected by a shorter PTT. Then, a reverse, compensatory effect occurs with the beat that follows. According to (8), this phenomenon explains the main difference between $d_{RR}(i)$ and $d_{pp}(i)$ that occurs at the first beat after a VPB (see Fig. 2).

C. Turbulence Onset

TO was the only one of the three parameters that exhibited a significant difference between $d_{RR}(i)$- and $d_{pp}(i)$-based analysis, and then only for N patients—a difference which is due to a shortened PTT that accompanies a VPB. In T patients, on the other hand, the baroreflex increases the heart rate so that the first beat after a VPB will arrive earlier, with less blood into the ventricles as a consequence. For T patients, the PTT is, therefore, shorter than it is before the VPB, although not as much as in N patients.

Since the influence of PTT is essentially isolated to the first interval after the VPB, an alternative definition of TO was tested in which the relative difference was computed between the average of the two normal intervals before the VPB and the average of the second and third normal intervals after the VPB. In the original definition of TO, the first and the second intervals are averaged instead. However, the modified TO was found to perform much worse than the original one since Acc dropped from 0.95 (cf., Table IV) to 0.77.

D. Turbulence Slope

The bias in TS is, just as for TO, caused by PTT-induced variability (cf., Fig. 2). To gain further insight on why bias occurs, the location of the window with the maximum slope was determined. In N patients, the index of the first beat in the window occurred earlier in $d_{pp}(i)$ than in $d_{RR}(i)$, the median beat index being $i = 6$ and $i = 10$, respectively. Furthermore, the variability of the beat index was found to be larger for $d_{pp}(i)$ than for $d_{RR}(i)$, with a standard deviation of 5.6 and 4.1, respectively. Thus, since the location of the maximum turbulence slope is closer to the VPB where PTT-induced variability is larger, TS computed from $d_{pp}(i)$ exhibits, in general, a larger value than the one computed from $d_{RR}(i)$.

In T patients, the influence of PTT increased the variability of the beat index in $d_{pp}(i)$-based analysis, whereas the median beat index remained the same for both types of analysis (3 ± 4.3 for $d_{pp}(i)$, 3 ± 1.3 for $d_{RR}(i)$). This result explains why the bias in TS is larger in N than in T patients (see Fig. 4).

E. T$_\Sigma$

The KL basis needed to compute T$_\Sigma$ was determined from the ECG, not the PPG, and from a group of patients completely

unrelated to this paper. The larger variability in T_Σ for T patients [see Fig. 4(c)] is explained by the fact that the KL basis is not matched to any of the present PPG databases. By choosing a KL basis which better reflects the PTT-related difference in the first few beats after the VPB, the performance can be expected to improve. For obvious reasons, the selection of basis is less critical in N patients than in T patients.

F. Limitations

Atrial premature beats were not considered in this paper. Since such beats may also cause HRT, PPG-based analysis would be of interest to perform. For example, the relationship between type of ectopic beat and the presence or absence of pulse in PPG signal and its value as marker of risk could be studied.

Since the present dataset is rather small, it is desirable to pursue a future study for the purpose of establishing the clinical significance of the PRT analysis.

VI. CONCLUSION

The results from the PPG- and ECG-based analysis of three different clinical contexts (hemodialysis treatment, intensive care monitoring, and EP study) suggest that the parameters TO, TS, and T_Σ can be computed from the PPG, and thus, serve as surrogates for the ECG-derived parameters. The PTT was found to have increased variability immediately after the VPB, influencing especially TO. PPG-based turbulence analysis may be considered in clinical applications where the ECG electrodes are inconvenient to wear or where oxygen saturation measurements are needed.

REFERENCES

[1] G. Schmidt, M. Malik, P. Barthel, R. Schneider, K. Ulm, L. Rolnitzky, A. J. Camm, J. T. Bigger, Jr., and A. Schomig, "Heart-rate turbulence after ventricular premature beats as a predictor of mortality after acute myocardial infarction," *Lancet*, vol. 353, pp. 1390–1396, 1999.

[2] A. Bauer, M. Malik, G. Schmidt, P. Barthel, H. Bonnemeier, I. Cygankiewicz, P. Guzik, F. Lombardi, A. Müller, A. Oto, R. Schneider, M. Watanabe, D. Wichterle, and W. Zareba, "Heart rate turbulence: Standards of measurement, physiological interpretation, and clinical use: International society for Holter and noninvasive electrophysiology consensus," *J. Amer. Coll. Cardiol.*, vol. 52, pp. 1353–1365, 2008.

[3] A. Bauer, P. Barthel, A. Müller, K. Ulm, H. Huikuri, M. Malik, and G. Schmidt, "Risk prediction by heart rate turbulence and deceleration capacity in postinfarction patients with preserved left ventricular function retrospective analysis of 4 independent trials," *J. Electrocardiol.*, vol. 42, no. 6, pp. 597–601, 2009.

[4] C. S. Zuern, P. Barthel, and A. Bauer, "Heart rate turbulence as risk-predictor after myocardial infarction," *Front Physiol.*, vol. 9, no. 2, 2011.

[5] M. Watanabe and G. Schmidt, "Heart rate turbulence: A 5-year review," *Heart Rhythm*, vol. 1, pp. 732–738, 2004.

[6] S. Abe, M. Yoshizawa, N. Nakanishi, T. Yazawa, K. Yokota, M. Honda, and G. Sloman, "Electrocardiographic abnormalities in patients receiving hemodialysis," *Amer. Heart J.*, vol. 131, pp. 1137–1144, 1996.

[7] C. Calvo, S. Maule, F. Mecca, R. Quadri, G. Martina, and P. C. Perin, "The influence of autonomic neuropathy on hypotension during hemodialysis," *Clin. Auton. Res.*, vol. 12, pp. 84–87, 2002.

[8] K. Solem, A. Nilsson, and L. Sörnmo, "An ECG-based method for early detection of abrupt changes in blood pressure during hemodialysis," *ASAIO J.*, vol. 52, pp. 282–290, 2006.

[9] A. Celik, M. Melek, S. Yuksel, E. Onrat, and A. Avsar, "Cardiac autonomic dysfunction in hemodialysis patients: The value of heart rate turbulence," *Hemodial. Int.*, vol. 15, pp. 193–199, 2011.

[10] L. Sörnmo, F. Sandberg, E. Gil, and K. Solem, "Noninvasive techniques for prevention of intradialytic hypotension," *IEEE Rev. Biomed. Eng.*, vol. 5, pp. 45–59, 2012.

[11] F. Javed, P. M. Middleton, P. Malouf, G. S. Chan, A. V. Savkin, N. H. Lovell, E. Steel, and J. Mackie, "Frequency spectrum analysis of finger photoplethysmographic waveform variability during haemodialysis," *Physiol. Meas.*, vol. 31, pp. 1203–1216, 2010.

[12] K. Solem, B. Olde, and L. Sörnmo, "Prediction of intradialytic hypotension using photoplethysmography," *IEEE Trans. Biomed. Eng*, vol. 57, no. 7, pp. 1611–1619, Jul. 2010.

[13] E. Mambelli, E. Mancini, and A. Santoro, "A continuous and non-invasive arterial pressure monitoring system in dialysis patients," *Nephron. Clin. Pract.*, vol. 107, pp. c170–c176, 2007.

[14] Y. Yan, C. Poon, and Y. Zhang, "Reduction of motion artifact in pulse oximetry by smoothed pseudo Wigner–Ville distribution," *J. Neuroeng. Rehabil.*, vol. 2, 2005.

[15] M. J. Hayes and P. R. Smith, "A new method for pulse oximetry possessing inherent insensitivity to artifact," *IEEE Trans. Biomed. Eng.*, vol. 48, no. 4, pp. 452–461, Apr. 2001.

[16] E. Gil, J. M. Vergara, and P. Laguna, "Detection of decreases in the amplitude fluctuation of pulse photoplethysmography signal as indication of obstructive sleep apnea syndrome in children," *Biomed. Signal Process Control*, vol. 3, pp. 267–277, 2008.

[17] B. Yang and K. H. Chon, "A novel approach to monitor nonstationary dynamics in physiological signals: Application to blood pressure, pulse oximeter, and respiratory data," *Ann. Biomed. Eng.*, vol. 38, no. 11, pp. 3478–3488, 2010.

[18] D. Zheng, J. Allen, and A. Murray, "Determination of aortic valve opening time and left ventricular peak filling rate from the peripheral pulse amplitude in patients with ectopic beats," *Physiol. Meas.*, vol. 29, pp. 1411–1419, 2008.

[19] G. B. Moody and R. G. Mark. (1996). A database to support development and evaluation of intelligent intensive care monitoring. *Comput. Cardiol.*, vol. 23, pp. 657–660, [Online]. Available: http://physionet.org/physiobank/database/mimicdb/

[20] D. Smith, K. Solem, P. Laguna, J. P. Martínez, and L. Sörnmo, "Model-based detection of heart rate turbulence using mean shape information," *IEEE Trans. Biomed. Eng.*, vol. 57, no. 2, pp. 334–342, Feb. 2010.

[21] J. P. Martínez, R. Almeida, S. Olmos, A. P. Rocha, and P. Laguna, "A wavelet-based ECG delineator: Evaluation on standard databases," *IEEE Trans. Biomed. Eng.*, vol. 51, no. 4, pp. 570–581, Apr. 2004.

[22] J. Mateo and P. Laguna, "Analysis of heart rate variability in the presence of ectopic beats using the heart timing signal," *IEEE Trans. Biomed. Eng.*, vol. 50, no. 3, pp. 334–343, Mar. 2003.

[23] F. van der Heijden, R. Duin, D. de Ridder, and D. Tax, *Classification, Parameter Estimation and State Estimation*. New York, NY, USA: Wiley, 2005.

[24] J. Y. A. Foo and C. S. Lim, "Pulse transit time as an indirect marker for variations in cardiovascular related reactivity," *Technol. Health Care*, vol. 14, pp. 97–108, 2006.

[25] J. P. Martínez, I. Cygankiewicz, D. Smith, A. Bayés de Luna, P. Laguna, and L. Sörnmo, "Detection performance and risk stratification using a model-based shape index characterizing heart rate turbulence," *Ann. Biomed. Eng.*, vol. 38, pp. 3173–3184, 2010.

[26] E. Gil, M. Orini, R. Bailón, J. M. Vergara, L. Mainardi, and P. Laguna, "Photoplethysmography pulse rate variability as a surrogate measurement of heart rate variability during non-stationary conditions," *Physiol. Meas.*, vol. 31, pp. 1271–1290, 2010.

Authors' photographs and biographies not available at the time of publication.